



A Mathematical Analysis of an In-vivo Ebola Virus Transmission Dynamics Model

Seleman Ismail^{1*} and Adeline Peter Mtunya²

¹Department of Physical Sciences, The Open University of Tanzania, Dar es Salaam, Tanzania.

²Department of Mathematics, Mkwawa University College of Education, University of Dar es Salaam, Iringa, Tanzania.

E-mails: seleman.ismail@out.ac.tz; mtunya_ap@muce.ac.tz; apmtunya@gmail.com

*Corresponding author:

Received 21 Jun 2021, Revised 30 Sep 2021, Accepted 27 Oct 2021, Published Oct 2021

DOI: <https://dx.doi.org/10.4314/tjs.v47i4.12>

Abstract

Ebola virus (EBOV) infection is a hemorrhagic and hazardous disease, which is among the most shocking threats to human health causing a large number of deaths. Currently, there are no approved curative therapies for the disease. In this study, a mathematical model for in-vivo Ebola virus transmission dynamics was analyzed. The analysis of the model mainly focused on the sensitivity of basic reproductive number, R_0 pertaining to the model parameters. Particularly, the sensitivity indices of all parameters of R_0 were computed by using the forward normalized sensitivity index method. The results showed that a slight change in the infection rate immensely influences R_0 while the same change in the production rate of the virus has the least impact on R_0 . Thus, R_0 , being a determining factor of the disease progression, deliberate control measures targeting the infection rate, the most positively sensitive parameter, are required. This implies that reducing infection rate will redirect the disease to extinction.

Keywords: Ebola virus infection, immune response, sensitivity index, mathematical model.

Introduction

Ebola virus (EBOV) is a single-stranded and negative sense RNA virus, which is a horrendously infectious, hemorrhagic and lethal disease, threatening to be a world tragedy to human health so far. The disease is among the most dangerous and shocking threats to human health, triggering a large number of deaths. It was first discovered in 1976 near Ebola River in Democratic Republic of Congo (DRC) (Fritz 2012, WHO 1978). Since then, over 20 outbreaks of EBOV infection have occurred in the world (Reece et al. 2016) and most of them appeared in South Sudan, Gabon Ivory Coast, South Africa and Uganda (CDC

2014). In West Africa, outbreaks of EBOV infection (EBOVI) emerged as well, which commenced in Guinea and later spread to Liberia and Sierra Leone; and by the end of 2014, the outbreak intensity had reached 13,268 cases. Of these, 27 cases had spread to neighboring and overseas countries in Senegal, Mali, Nigeria, Spain and United States (WHO Ebola Response Team 2014). Recently, outbreaks of EBOVI have relapsed in the eastern part of DRC, threatening to spread to neighboring and nearby countries such as Cameroon, Uganda, Rwanda, Burundi, Kenya, Tanzania, Zambia, Congo and South Sudan. Outbreaks of EBOVI in Central and East

African countries have not been significantly experienced though most of them, being neighboring countries to DRC, are at risks of the disease outbreaks.

The incubation period of EBOV ranges from 2 to 21 days and the infectious period ranges from 4 to 10 days. In the meantime, it takes about 31 days to quarantine a patient for investigation of the virus. The virus impairs an enormous variety of cell types including monocytes, macrophages, dendritic cells, endothelial cells, fibroblasts, hepatocytes and several types of epithelial cells; but it primarily targets the dendritic cells, monocytes and macrophages cells (CDC 2014). It is frequently hypothesized that EBOV infection arouses lymphocyte apoptosis that deters development of an effective adaptive immune response, which causes overwhelming state and subsequent death.

The EBOV can be transmitted from animal to animal, human to human and animal to human. It can be transmitted from bats to other animals, usually gorillas, chimpanzees and baboons (Acha and Szyfres 2003). It can also be transmitted to humans by contact with body fluids of the animals; and susceptible humans can be infected through direct contact with the saliva, mucus, vomit, faeces, sweat, tears, breast milk, urine and semen of infected people. EBOVI is typically manifested by headache, fever, vomiting, bleeding, diarrhea and rash (Fauci 2014); and in an infected person, severe bleeding and shock follows, which causes death. The risk of death from EBOVI is about 60% and increases as the infection progresses to the hemorrhage (bleeding) stage; and an infected individual becomes infectious at this stage. On the other hand, the transmission of the virus and subsequent death of infected people largely reduces through early discovery and effective contact tracing (Beeching et al. 2014).

Presently, there are no approved therapies specific for EBOV infections (Wong and Uyeki 2015). The major strategies currently used in the treatment of the disease are confined to symptomatic and supportive care of infected

individuals, by maintaining fluids, electrolytes and acid-base balance of blood, and treatment of secondary infections (Tseng and Chan 2015).

Mathematical modeling has played a substantial role in understanding the dynamics of different virus infections (Nowak and May 2000). Amongst existing models, the most prevalent dynamics models are HIV (Kirschner 1996, Duffin and Tullis 2002, Perelson 2002, Hernandez-Vargas et al. 2011, Hernandez-Vargas and Middleton 2013); hepatitis virus (Ribeiro et al. 2002, Reluga et al. 2009, Guedj et al. 2013); influenza virus (Baccam et al. 2006, Handel et al. 2010, Smith and Perelson 2011, Pawelek et al. 2012, Hernandez-Vargas et al. 2014). Literatures show that several mathematical models have been developed to investigate the transmission dynamics of EBOV in human populations and human cell populations. But, there exist few mathematical models that describe the virus transmission dynamics in vivo with different dynamical effectors (Wester 2015, Martyushev et al. 2016, Lasisi et al. 2018), which accounts for inadequate understanding of the virus dynamics. This advocates the necessity for further research in order to fully understand it. Thus, in this article, a deterministic mathematical model is formulated to study the effect of weakened response of cytotoxic T-lymphocytes on the transmission dynamics of EBOV.

Materials and Methods

Model formulation and description of dynamics

In this section, a mathematical model for the in-vivo transmission of EBOV is formulated. The model is developed to study the transmission dynamics of the virus in an infected human body. It consists of heterogeneous populations, which are classified as uninfected cells (U), infected cells (I) cytotoxic T-lymphocytes (Z) and Ebola viruses (B). Uninfected cells, U , are increased by a production rate Π and die naturally at a rate

$\alpha_1 U$. Free viruses, B , interact with uninfected cells at a rate βBU progressing to the infected cells class; and die naturally at a rate $\alpha_1 I$. Also, they attack cytotoxic T-lymphocytes exterminating them at a rate μBZ . Infected cells reproduce free viruses at a rate ωI , which die naturally at a rate $\alpha_2 B$. Cytotoxic T-lymphocytes increase by a rate λZ , kill infected cells at a rate σIZ and die naturally at a rate $\alpha_3 Z$.

The following assumptions guided the formulation of the model:

- i. Uninfected cells are produced at a constant rate.
- ii. Uninfected cells are equally likely infected by the virus.
- iii. Uninfected cells and infected cells die naturally at equal constant rates.
- iv. Viruses are produced from infected cells at a constant rate.
- v. Viruses die naturally at a constant rate.
- vi. Cytotoxic T-lymphocytes are produced and die naturally at constant rates.
- vii. Cytotoxic T-lymphocytes eliminate infected cells at a constant rate.
- viii. The virus wipes out cytotoxic T-lymphocytes at a constant rate.

For simplicity of analyses and discussions, the model variables are usually expressed as U , I , B and Z to represent the population sizes $U(t)$, $I(t)$, $B(t)$ and $Z(t)$ at time t , respectively. Besides, these variables and all model parameters are briefly described in Table 1 and Table 2, respectively.

Table 1: Variables of the model

Variable	Description
$U(t)$	Number of uninfected cells
$I(t)$	Number of infected cells
$B(t)$	Number of infectious viruses
$Z(t)$	Number of cytotoxic T-lymphocytes

Table 2: Parameters of the model

Parameter	Description
α_1	Natural death rate of uninfected cells and uninfected cells
α_2	Natural death rate of the virus
α_3	Natural death rate of cytotoxic T-lymphocytes
μ	Eradication rate of cytotoxic T-lymphocytes
Π	Reproduction rate of uninfected cells
β	Infection rate of uninfected cells
λ	Reproduction rate of cytotoxic T-lymphocytes
ω	Reproduction rate of the virus
σ	Clearance rate of infected cells by cytotoxic T-lymphocytes

Model flow diagram

The transmission dynamics of EBOV can be illustrated with a model flow diagram as

shown in Figure 1, where the role of each dynamic effector can be easily conceived.

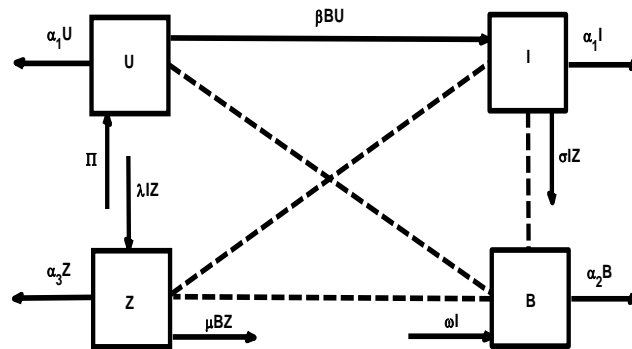


Figure 1: Model flow diagram for in-vivo EBOV dynamics.

Equations of the model

The dynamics of Ebola virus, having been thoroughly described and briefly illustrated in a flow diagram, can further be represented by a system of non-linear ordinary differential equations. At this juncture, the model system has Equations (1) –(4), which model uninfected cells population, infected cells population, virus population and cytotoxic T-lymphocytes population. Therefore, the system of equations is hereby presented.

$$\frac{dU}{dt} = \Pi - \beta BU - \alpha_1 U \quad (1)$$

$$\frac{dI}{dt} = \beta BU - \sigma IZ - \alpha_1 I \quad (2)$$

$$\frac{dB}{dt} = \omega I - \alpha_2 B \quad (3)$$

$$\frac{dZ}{dt} = \lambda IZ - \mu BZ - \alpha_3 Z \quad (4)$$

and initial conditions: $U(0) = U_0$, $I(0) = I_0$, $B(0) = B_0$, and $Z(0) = Z_0$

Basic properties of the model

Here, the basic properties of the model are presented. Systematic discussions have been made to verify non-negativity of the model state variables for all $t \geq 0$, assuming that the model parameters are all positive. Also, the invariant region (domain) that contains all

feasible solutions of the model system variables has been determined.

Positivity of solutions

Since the system (1) - (4) models heterogeneous populations, all state variables and parameters must be non-negative for all $t \geq 0$. Then the required task, here, is to attest that the variables $U(t)$, $I(t)$, $B(t)$ and $Z(t)$ are nonnegative for all $t \geq 0$. This has been done through Lemma 1.

Lemma 1: Given a model system with initial values $\{U(0), I(0), B(0), Z(0) \in R_+^5\}$, the solution set $\{U(t), I(t), B(t), Z(t)\}$ contains nonnegative values for all $t \geq 0$.

Proof:

At this juncture, the proof means analytical process of verifying the positivity of the model state variables for all $t \geq 0$. Thus, from the model system of Equations (1) - (4), the following results have been obtained:

(i) Ebola virus population

From Equation (3), the result is given by

$$\frac{dB}{dt} \geq -\alpha_2 B \quad (5)$$

Integrating Equation (5) with respect to time t produces

$$\ln B(t) \geq -\alpha_2 t + K_1, \quad (6)$$

where K_1 is a constant.

Then the general solution of Equation (6) is

$$B(t) \geq B_0 \exp(-\alpha_2 t),$$

where B_0 represents the initial size of Ebola viruses population.

This implies that

$$B(t) \geq B_0 \exp(-\alpha_2 t) \geq 0, \quad (7)$$

(ii) Uninfected cells population

Considering (1), the result is

$$\frac{dU}{dt} \geq -\beta BU - \alpha_1 U \quad (8)$$

Integrating Equation (8) with respect to time t produces

$$\ln U \geq \int_0^t (-\beta B(s) - \alpha_1) ds + K_3, \quad (9)$$

where K_3 is a constant.

Then the general solution of Equation (9) is

$$\ln U \geq U_0 \exp \left[\int_0^t (-\beta B(s) - \alpha_1) ds \right],$$

where U_0 represents the initial size of uninfected cells population

This implies that

$$\ln U \geq U_0 \exp \left[\int_0^t (\beta B(s) - \alpha_1) ds \right] \geq 0 \quad (10)$$

(iii) Cytotoxic T lymphocytes population

Analysis of Equation (4) produces

$$\frac{dZ}{dt} \geq (\phi B - \alpha_3) Z \quad (11)$$

Integrating Equation (11) with respect to time t produces

$$\ln Z \geq \int_0^t (\phi B(s) - \alpha_3) ds + K_3, \quad (12)$$

where K_4 is a constant.

Then the general solution of Equation (12) is

$$Z(t) \geq Z_0 \exp \left[\int_0^t (\phi B(s) - \alpha_3) ds \right],$$

where Z_0 represents the initial size of cytotoxic T lymphocytes population

This implies that

$$Z(t) \geq Z_0 \exp \left[\int_0^t (\phi B(s) - \alpha_3) ds \right] \geq 0 \quad (13)$$

(iv) Infected cells population

Analysis of Equation (2) produces

$$\frac{dI}{dt} \geq -\sigma I - \alpha_1 I \quad (14)$$

Integrating Equation (14) with respect to time t produces

$$I(t) \geq \int_0^t (-\sigma Z(s) - \alpha_1) ds + K_5 \quad (15)$$

where K_5 is a constant.

Then the general solution of (15) is

$$I(t) \geq I_0 \exp \left[\int_0^t (-\sigma Z(s) - \alpha_1) ds \right] \geq 0,$$

where I_0 represents the initial size of infected cells population.

This implies that

$$I(t) \geq I_0 \exp \left[\int_0^t (-\sigma Z(s) - \alpha_1) ds \right] \geq 0 \quad (16)$$

Hence the results (7), (10), (13) and (16) validate that set $\{U(t), I(t), B(t), Z(t)\}$ comprises non-negative values. In respect of this, the model (1) - (4) is epidemiologically and mathematically realistic (Hethcote 2000).

Invariant regions

Since the system of non-linear differential Equations (1) - (4) involves modeling of target cells population, Ebola viruses population and cytotoxic T lymphocytes population, it is assumed that the model variables and parameters are non-negative for all $t \geq 0$. At this stage, an invariant region for the model containing all feasible solutions is determined. This is achieved through Lemma 2.

Lemma 2: All forward solutions of the model system (1) - (4), are contained in the region

$$\Lambda \subset R_+^4, \forall t \geq 0,$$

where $\Lambda = \psi_N \times \psi_B \times \psi_Z$, in which

$$\psi_N = \{(U, I) \in R_+^2 : U + I \leq N\},$$

$$\psi_B = \{B \in R_+^1 : (4) \text{ is satisfied}\}$$

$$\psi_Z = \{Z \in R_+^1 : (4) \text{ is satisfied}\}$$

where Λ is a positive invariant region for the whole system (1) - (4).

Proof

Here, the invariant region for the whole system has been established by initially determining the bounded regions for individual populations.

(i) Target cells population

In this case, the bounded region containing all possible solutions for the target cells population is determined, Let ψ_N be the

bounded region; and let $\psi_N = (U, I) \in R_+^2$ be any solution of the system with non-negative initial conditions U_0 and I_0 for all $t \geq 0$.

Then, the variables: N , U and I are related in the following manner:

$$N(t) = U(t) + I(t) \tag{17}$$

where N denotes the target cells population size at time t .

This implies that

$$\frac{dN}{dt} = \frac{dU}{dt} + \frac{dI}{dt} \tag{18}$$

Substituting Equations (1) and (2) into Equation (18) produces

$$\frac{dN}{dt} = \Pi - \alpha_1 N - \sigma IZ \tag{19}$$

This further produces

$$\frac{dN}{dt} \leq \Pi - \alpha_1 N, \tag{20}$$

Integrating Equation (20) with respect to t produces

$$N(t) \leq \frac{\Pi}{\alpha_1} + K_6 \exp(-\alpha_1 t), \tag{21}$$

where K_6 is a constant.

Hence the general solution of Equation (21) is:

$$N(t) \leq \frac{\Pi}{\alpha_1} + \left(N_0 - \frac{\Pi}{\alpha_1}\right) \exp(-\alpha_1 t) \tag{22}$$

where U_0 denotes the initial quantity of target cells population evaluated at the initial conditions $U_0 = U(0) \geq 0$ and $I_0 = I(0) \geq 0$.

Analysis of Equation (22) results in the following two cases at $t \geq 0$.

Case 1: If $N_0 > \frac{\Pi}{\alpha_1}$, the largest value of right

hand side (RHS) of Equation (22) is obtained at $t = 0$; and the value is N_0 . Thus, $N(t) \leq N_0$

Case 2: If $N_0 < \frac{\Pi}{\alpha_1}$, the value

$\left(N_0 - \frac{\Pi}{\alpha_1}\right) \exp(-\alpha_1 t)$ is negative and tends to zero as $t \rightarrow \infty$. So, the largest value in the RHS of Equation (22) is $\frac{\Pi}{\alpha_1}$. Thus, $N(t) \leq \frac{\Pi}{\alpha_1}$

This implies that

$$N(t) \leq \max\{N_0, N^*\}, \forall t \geq 0 \text{ and whatever}$$

value of N_0 , where $N^* = \Pi/\alpha_1$. So, $N(t)$ is bounded above.

Thus, all possible solutions for the target cells population are contained in the region ψ_N , where:

$$\psi_N = \{N(t) : N(t) \leq N^*\}, \forall t \geq 0 \tag{23}$$

(ii) Ebola virus population

At this point, the bounded region containing all possible solutions for Ebola virus population is determined. Let ψ_B be the bounded region; and

let $\psi_B = (B) \in R_+^1$ be any solution of the system with non-negative initial conditions B_0 for all $t \geq 0$.

Analysis of Equation (3) with Equation (23) produces

$$\frac{dB}{dt} \leq \omega N^* - \alpha_2 B \tag{24}$$

Here, a bounded region containing all possible solutions for cytotoxic T-lymphocytes population has been determined. Let ψ_z be the bounded region; and let $\psi_Z = (Z) \in R_+^1$ be any solution of the system with non-negative initial condition Z_0 for all $t \geq 0$.

Then Equation (4), with Equations (23) and (24), change to

$$\frac{dZ}{dt} \leq \lambda N^* Z - \phi B^* Z - \alpha_3 Z \quad (25)$$

Integrating Equation (25) with respect to t produces

$$\ln Z \leq K_8 \exp((\lambda N^* - \phi B^* - \alpha_3)t), \quad (26)$$

where K_8 is a constant.

The general solution of Equation (26) is

$$Z(t) \leq Z_0 \exp((\lambda N^* - \phi B^* - \alpha_3)t), \quad (27)$$

where Z_0 denotes the initial quantity of cytotoxic T-lymphocytes population.

If $\lambda N^* - \phi B^* - \alpha_3 > 0$, analysis of (27) is achieved through two cases, which are:

Case 1: The value of the right hand side (RHS) of (27) obtained at $t = 0$ is Z_0 .

Case 2: The value $Z_0 \exp((\lambda N^* - \phi B^* - \alpha_3)t)$ in the RHS of (27) becomes positively larger as $t \rightarrow \infty$.

This implies that $Z(t)$ has a lower bound.

Hence all possible solutions for Ebola virus population are contained in the region ψ_Z , where

$$\psi_Z = \{Z(t) : Z(t) \geq Z_0\}, \quad \forall t \geq 0 \quad (28)$$

Thus, the invariant region for the entire system (1) - (4) is given by

$$\Lambda = \psi_N \times \psi_B \times \psi_Z,$$

where $\psi_N = \{N(t) : N(t) \leq N^*\}$,

$$\psi_B = \{B(t) : B(t) \leq B^*\}$$

and $\psi_Z = \{Z(t) : Z(t) \geq Z_0\}, \forall t \geq 0$.

Results and Discussion

In this section, the model is systematically analyzed to produce some fundamental results: disease free equilibrium, E_0 , and basic reproductive number R_0 , which is also known as basic reproductive ratio (BRR). Here, the sensitivity of BRR relating to the model parameters is performed as well.

Disease free equilibrium:

Definition 1: Disease free equilibrium, E_0 , is a state of dynamic equilibrium that describes the absence of an infectious disease in a susceptible population (in this case, human target cells).

Analytically, this is obtained by making the differential coefficients of the model variables equal to zero. That is,

$$\frac{dU}{dt} = \frac{dI}{dt} = \frac{dB}{dt} = \frac{dZ}{dt} = 0 \quad (29)$$

This implies that

$$\begin{cases} \Pi - \beta UB - \alpha_1 U = 0 \\ \beta UB - \sigma IZ - \alpha_1 I = 0 \\ \omega I - \alpha_2 B = 0 \\ \lambda IZ - \phi BZ - \alpha_3 Z = 0 \end{cases} \quad (30)$$

In the absence of disease, the human cells population becomes virus-free ($B = 0$), which implies no production of infected cells ($I = 0$). Besides, the cytotoxic T-lymphocytes are not produced ($Z = 0$) in the absence of infected cells. Therefore, the system remains merely with susceptible target cells, implying that the variable U takes a non-zero value ($U \neq 0$). This is obtained from the first equation of the system (33) and given by

$$\Pi - \beta BU - \alpha_1 U = 0 \Rightarrow \Pi \times \beta \times 0 - \alpha_1 U = 0$$

$$\Rightarrow \Pi - \alpha_1 U = 0$$

This produces $U = \frac{\Pi}{\alpha_1}$.

Hence the system becomes free from disease at

$$E_0 = (U^0, I^0, B^0, Z^0) = \left(\frac{\Pi}{\alpha_1}, 0, 0, 0 \right)$$

Basic reproductive number, R_0

Definition 2: The basic reproduction number, R_0 , is the expected number of secondary cases produced by a typical infected individual during its entire infectious period, in population consisting of only susceptible individuals (Heesterbeek and Dietz 1996). In this case, it can be defined as the expected number of secondary infections generated by a single infected cell in a susceptible target cells population during its infectious period.

The quantity R_0 describes the ability of an infectious disease to attack susceptible individuals. It explains the disease dynamical behaviour, where $R_0 < 1$ means the disease cannot establish itself in the population; only a small number of individuals are infected. But, if $R_0 > 1$, there is a possibility of a larger disease outbreak and prevails in a population. Besides, it is a measure to determine the amount of efforts required for a given control measure to eradicate an epidemic.

This can be obtained by the method of next generation matrix (Diekmann and Heesterbeek 2000, Van den Driessche and Watmough 2002) as follows:

If we assume F as a non-negative $m \times m$ matrix and V as a non-singular

M - matrix such that $F = \left[\frac{\partial F_i(E_0)}{\partial x_j} \right]$

and $V = \left[\frac{\partial V_i(E_0)}{\partial x_j} \right]$ with $1 \leq i, j \leq m$

where F_i is the occurrence of new infections in compartment i , $V_i = V_i^- - V_i^+$ in which V_i^+ is the rate of transfer of entities into compartment i by all other means while V_i^- is the rate of transfer of entities out of compartment i and E_0 is the disease free equilibrium point, it follows that the effective reproductive number R_0 is the spectral radius (dominant eigenvalue) of the matrix FV^{-1} , which is denoted by $R_0 = \rho(FV^{-1})$.

Rearranging the equations of the system (1) - (4) in such a way that the infectious classes occur first, produces a system of equations of the form:

$$x'_i = f_i(x) = F_i(x) - V_i(x), i = 1, 2, \dots, n$$

At this juncture, it is assumed that each function f_i is continuous and at least twice differentiable in the region defined by Λ . Then F_i and V_i are derived as follows:

$$F_i = \begin{bmatrix} f_1 \\ f_2 \end{bmatrix} = \begin{bmatrix} \beta B U \\ \omega I \end{bmatrix} \text{ and } V_i = \begin{bmatrix} v_1 \\ v_2 \end{bmatrix} = \begin{bmatrix} \sigma Z I + \alpha_1 I \\ \alpha_2 B \end{bmatrix}$$

Thus, the Jacobean matrices F and V at E_0 are given by

$$F = \frac{\partial F_i(E_0)}{\partial X_j} = \begin{pmatrix} 0 & \beta U^0 \\ \omega & 0 \end{pmatrix} = \begin{pmatrix} 0 & \frac{\beta \Pi}{\alpha_1} \\ \omega & 0 \end{pmatrix}$$

$$F = \frac{\partial F_i(E_0)}{\partial X_j} = \begin{pmatrix} 0 & \frac{\beta \Pi}{\alpha_1} \\ \omega & 0 \end{pmatrix} \tag{31}$$

$$V = \frac{\partial V_i(E_0)}{\partial X_j} = \begin{pmatrix} \alpha_1 + \sigma Z^0 & 0 \\ 0 & \alpha_2 \end{pmatrix} = \begin{pmatrix} \alpha_1 & 0 \\ 0 & \alpha_2 \end{pmatrix}$$

$$V = \frac{\partial V_i(E_0)}{\partial X_j} = \begin{pmatrix} \alpha_1 & 0 \\ 0 & \alpha_2 \end{pmatrix} \tag{32}$$

The inverse of (35) is given by

$$V^{-1} = \frac{1}{\alpha_1 \alpha_2} \begin{pmatrix} \alpha_2 & 0 \\ 0 & \alpha_1 \end{pmatrix} = \begin{pmatrix} \frac{1}{\alpha_1} & 0 \\ 0 & \frac{1}{\alpha_2} \end{pmatrix} \tag{33}$$

Multiplication of (31) and (33) produces

$$FV^{-1} = \begin{pmatrix} 0 & \frac{\beta \Pi}{\alpha_1 \alpha_2} \\ \frac{\omega}{\alpha_1} & 0 \end{pmatrix}$$

The characteristics equation of FV^{-1} is given by $|(FV^{-1}) - \lambda| = 0$, implying that

$$\begin{vmatrix} -\lambda & \frac{\beta \Pi}{\alpha_1 \alpha_2} \\ \frac{\omega}{\alpha_1} & -\lambda \end{vmatrix} = 0$$

The largest eigenvalue (the spectral radius of FV^{-1}) is

$$\lambda = \sqrt{\frac{\omega\beta\Pi}{\alpha_1^2\alpha_2}}$$

Thus, the basic reproductive number, R_0 is given by

$$R_0 = \sqrt{\frac{\omega\beta\Pi}{\alpha_1^2\alpha_2}} \quad (34)$$

The analytical result (34) shows that the value of R_0 at time $t \geq 0$ depends on infection rate, virus production rate, production rate of susceptible cells and natural death rates of uninfected cells, infected cells and virus. On the other hand, the immune system does not determine disease progression as the parameter for cytotoxic T-lymphocytes is not embedded in R_0 .

Sensitivity analysis

At this juncture, it is necessary to perform an investigation to realize how sensitive the threshold quantity basic reproduction number, R_0 is with regard to its parameters. This analysis tells us how crucial and important each of the parameters is to the disease transmission. Particularly, this focuses on finding sites in the disease dynamics where intervention strategies can be directed to. This will assist scientists in the making of new drugs and pharmacists in

choosing a suitable therapeutic prescription for preventing and controlling the disease transmission in-vivo. This is accomplished through normalized forward sensitivity index method, where the sensitivity index of R_0 relating to each parameter embedded in it is calculated.

Definition 3: If a variable C depends differentially on a parameter W , then the normalized forward sensitivity index of C with respect to W is denoted by X_C . This is defined as:

$$X_W^C = \frac{C}{W} \times \frac{\partial W}{\partial C} \quad (35)$$

Removing C for R_0 in (35) and then performing computations results in an expression for the sensitivity of R_0 with respect to W . This is

$$X_W^{R_0} = \frac{W}{R_0} \times \frac{\partial R_0}{\partial W} \quad (36)$$

In this study, the method and the threshold quantity parameters have been used to calculate the sensitivity indices of R_0 , where almost all parameter values have been adopted from literatures and are itemized in Table 3.

Table 3: Parameter values used for sensitivity analysis

Parameter	Value	Unit	References
Π	5.05	Cell/ml/day	Wester 2015
β	0.1	Cell/ml/day	CDC 2014
ω	40.9	Virus cell ⁻¹ day ⁻¹	Wester 2015
λ	0.1	Cell/ml/day	Banton et al. 2010
σ	0.1	Cell/day	Wester 2015
α_1	0.5	Cell/day	Estimated
α_2	1.15	Cell/day	Nguyen et al. 2015
α_3	0.5	Cell/day	Wester 2015
μ	0.1	Cell/day	Estimated

The sensitivity index of R_0 with respect a specific model parameter is normally obtained by replacing W in (36) with the parameter. This is accomplished by substituting the corresponding parameter value in the resulting expression and then performing computation. Thus, in this study, the sensitivity index of R_0 with respect to every parameter (embedded in R_0) is calculated using parameter values itemized in Table 3. Then the resulting indices, corresponding to the threshold quantity parameters, are altogether enumerated in Table 4.

Table 4: Sensitivity of R_0 relating to model parameters

Parameter	Sensitivity index
β	42.3798
α_1	-16.9519
α_2	-3.6852
Π	0.8392
ω	0.1036

In Table 4, it is observed that the parameter for the virus production rate β is most sensitive, followed by the parameter for natural death rate of human cells α_1 , followed by the parameter for the natural death rate of the virus α_2 while the parameter of infection rate ω is least sensitive one. That is,

$$X_{\beta}^{R_0} > X_{\alpha_1}^{R_0} > X_{\alpha_2}^{R_0} > X_{\Pi}^{R_0} > X_{\omega}^{R_0}$$

Note that the absolute value of a particular sensitivity index has been used for the comparison.

It is further observed that the parameter for the virus production rate is most positively sensitive, while the parameter for infection rate is the least positively sensitive one. Conversely, the parameter for natural death rate of human cells is most negatively, while the parameter for natural death rate of the virus is

the least negatively sensitive one. This suggests that an increase of the virus production rate by 100% triggers a corresponding increase of R_0 by 4237.9% and vice versa. Conversely, a decrease of the virus natural death rate by 10% causes a corresponding increase of R_0 by 36.9% and vice versa.

Numerical simulations

For further understanding of the dynamical behaviour of the model system (1) - (4) at various situations, numerical simulations have been performed. This has been achieved using the parameter values itemized in Table 3. Here, variations of the basic reproduction number R_0 with respect to all parameters it contains are illustrated, which substantiates the analytical results obtained in the previous section.

Figures 2, 3 and 4 illustrate variations of the basic reproductive number, R_0 with respect to parameters: infection rate, β ; virus production rate, ω and production rate of uninfected human cells, Π , respectively. This implies the parameters β , ω and Π are proportional to R_0 , which means that an increase of the value of β , ω or Π causes an increase of R_0 and vice versa. Epidemiologically, the increase of R_0 means more uninfected cells get infected and ultimately the disease becomes prevalent in the body, while the decrease of it implies the number of infected cells reduces, which can result in the disease extinction in the long run. On the contrary, Figures 5 and 6 show variations of R_0 with natural death rate of human cells, α_1 and natural death rate of the virus, α_2 respectively. It is observed that an upsurge of the value of α_1 or α_2 triggers a decrease of R_0 and vice versa.

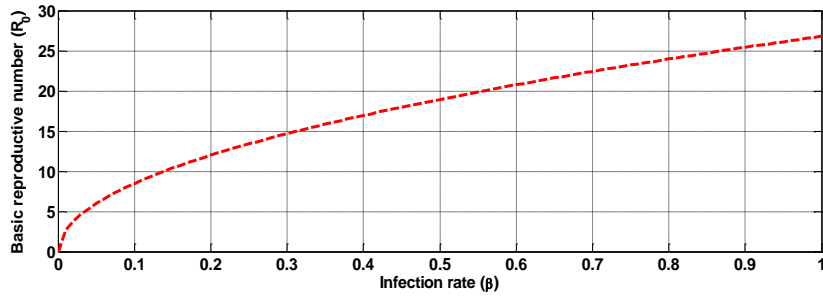


Figure 2: Variation of the basic reproduction number R_0 with infection rate β .

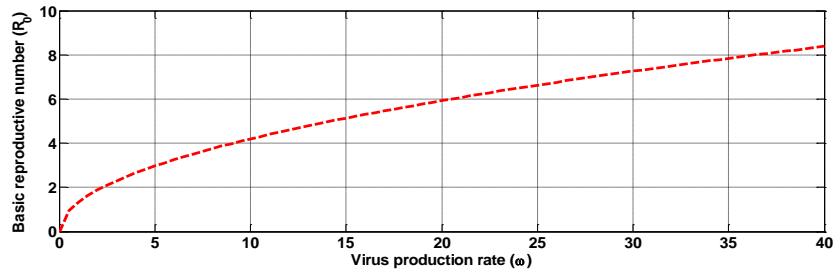


Figure 3: Variation of the basic reproduction number R_0 with virus production rate ω .

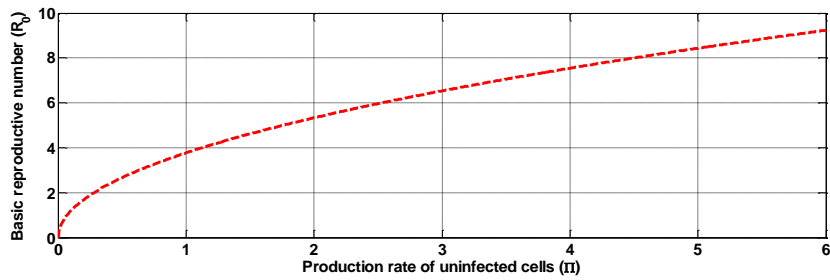


Figure 4: Variation of the basic reproduction number R_0 with production rate of uninfected cells Π

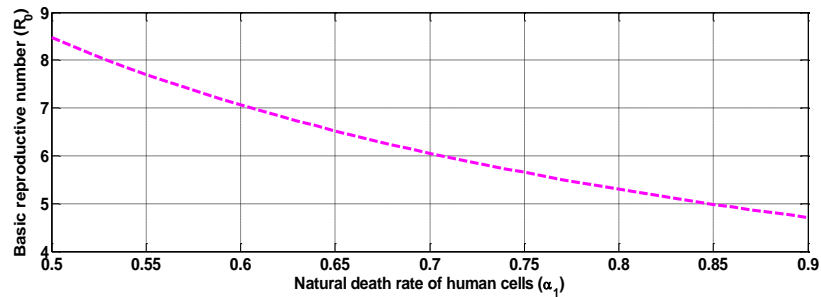


Figure 5: Variation of basic reproduction number R_0 with natural death rate of human cells α_1 .

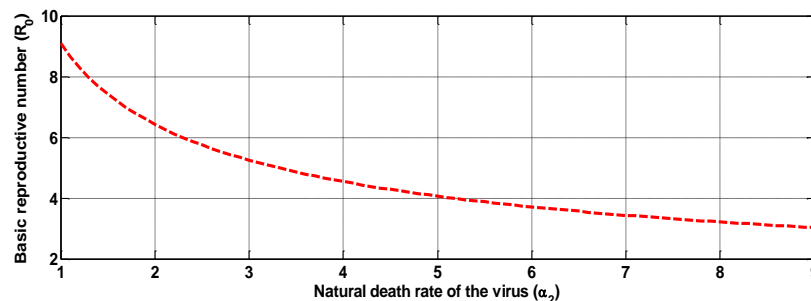


Figure 6: Variation of basic reproduction number R_0 with natural death rate of the virus α_2 .

Conclusion

This study has presented a deterministic mathematical model to study the transmission dynamics of Ebola virus in vivo. The analysis of the model has provided extra understanding of the disease natural course during infections and facilitated identification of sites in the dynamics that can be potentially targeted for intervention. The results indicate that the model is both mathematically and epidemiologically realistic as all variables of the model have been proven to be non-negative for all $t \geq 0$, assuming that all parameters are positive. Moreover, the model system of equations were used to find the state of no disease at equilibrium, that is represented by $E_0 = (\Pi/\alpha_1, 0, 0, 0)$, meaning that the system consists of only uninfected target cells at this state.

At disease free equilibrium, E_0 , the threshold quantity R_0 is computed, which describes the disease progress. The quantity R_0 depends on the infection rate, virus production rate, production rate of target cells, natural death rate of target cells and infected cells, and natural death rate of Ebola virus. On the other hand, the immune response does not determine the disease progression though it plays a foremost role in the entire disease dynamics. This is attributable to absence of the parameter for cytotoxic T-lymphocytes in R_0 . Also, sensitivity analysis has been performed with normalized forward sensitivity index method, where the sensitivity index of each

parameter of R_0 has been calculated. The results indicate that the parameter for infection rate β has the greatest index, while the parameter for virus production rate ω has the least index. This implies that a slight change of β triggers a considerable change of R_0 , which varies slightly as ω varies a little. Numerical simulations are performed as well, which substantiate the analytical results.

In this study, the sensitivity analysis provides further understanding of the in-vivo dynamics of EBOV. Since a slight change of the parameter with greatest sensitivity index prompts a drastic change in the disease progression, special attention should be directed to it. Consequently, it is recommended that deliberate control measures should be taken targeting on the rate of infection. The control measures are expected to decrease infection rate, and therefore redirect the disease to extinction.

Acknowledgements

The authors of this article would like to express sincere gratitude to the Management of Dodoma Regional Government Hospital (MDRGH) for being incredibly cooperative. Through MDRGH, we could contact doctors and other medical experts to obtain all necessary information regarding Ebola virus infections. This facilitated our research work a good deal.

Declaration

The authors declare that there is no conflict of interest whatsoever regarding this research work.

References

- Acha PN and Szyfres B 2013 Zoonoses and Communicable Diseases Common to Man and Animals, 3rd edition. Pan American Health Organization.
- Baccam P, Beauchemin C, Macken CA, Hayden FG and Perelson AS 2006 Kinetics of influenza A virus infection in humans. *J. Virol.* 80(15): 7590-7599.
- Beeching NJ, Fenech M and Houliham CF 2014 Ebola virus disease. *BMJ: Clinical Review* 349: g7348.
- Banton S, Roth Z and Pavlovic M 2010 Mathematical modeling of Ebola virus dynamics as a step towards rational vaccine design. In 26th Southern Biomedical Engineering Conference SBEC 2010, April 30-May 2, 2010, College Park, Maryland, USA (pp. 196-200). Springer, Berlin, Heidelberg.
- CDC 2014 CDC report to Ebola virus disease. 63(50): 1199-1201.
- Diekmann O and Heesterbeek, JAP 2000 Mathematical Epidemiology of Infectious Diseases: Model Building, Analysis and Interpretation, Wiley, New York, USA.
- Duffin RP and Tullis RH 2002 Mathematical models of the complete course of HIV infection and AIDS. *J. Theor. Med.* 4(4): 215-221.
- Fauci AS 2014 Ebola underscoring the global disparities in health care resources. *New Engl. J. Med.* 371(12): 1084-1086.
- Fritz E 2012 Innate immune response to Ebola virus infection. https://www.bdbiosciences.com/documents/Grant_E_Fritz.pdf (Accessed on 12/03/2020)
- Guedj J, Dahari H, Rong L, Sansone ND, Nettles RE, Cotler SJ, Leyden TJ, Uprichard SL and Perelson AS 2013 Modeling shows that the NS5A inhibitor daclatasvir has two modes of action and yields a shorter estimate of the hepatitis C virus half-life, *Proceedings of the National Academy of Sciences of United States of America* 110(10): 3991-3996, USA.
- Handel A, Longini IM and Antia R 2010 Towards a quantitative understanding of the within-host dynamics of influenza A infections. *J. Soc. Interface* 7(4): 35-47.
- Heesterbeek JAP and Dietz K 1996 The concept of R_0 in epidemic theory. *Stat. Neerl.* 50(1): 89-110.
- Hernandez-Vargas E, Colaneri P, Middleton R and Blanchini F 2011 Discrete-time control for switched positive systems with application to mitigating viral escape. *Int. J. Robust Nonlinear Control* 21(10): 1093-1111.
- Hernandez-Vargas EA and Middleton RH 2013 Modeling the three stages in HIV infection. *J. Theor. Biol.* 320: 33-40.
- Hernandez-Vargas EA, Wilk E, Canini L, Toapanta FR, Binder SC, Uvarovskii A, Ross TM, Guzman, CA, Perelson AS and Meyer-Hermann M 2014 Effects of aging on influenza virus infection dynamics. *J. Virol.* 88(8): 4123-4131.
- Kirschner D 1996 Using mathematics to understand HIV immune dynamics. *Not. Am. Math. Soc.* 43(2): 191-202.
- Lasisi NO, Akinwande NI, Olayiwola RO and Cole AT 2018 Mathematical model for Ebola virus infection in human with effectiveness of drug usage. *J. Appl. Sci. Environ. Manag.* 22(7): 1089-1095.
- Martyushev A, Nakaoka S, Sato K, Noda T and Lwami S 2016 Modeling Ebola virus dynamics: Implications for therapy. *Antiviral Res.* 135: 62-73.
- Nguyen VK, Binder SC, Boianelli A, Meyer-Hermann M, Hernandez-Vargas EA 2015 Ebola virus infection modeling and identifiability problems. *Front. Microbiol.* 6: 257.
- Nowak MA and May R 2000 Virus Dynamics: Mathematical Principles of Immunology and Virology, Vol. 291, Oxford University Press, Oxford, UK.
- Pawelek KA, Huynh GT, Quinlivan M, Cullinane A, Ron L, and Perelson AS 2012

- Modeling within-host dynamics of influenza virus infection including immune responses. *PLoS Comput. Biol.* 8(6): e1002588.
- Perelson AS 2002 Modeling viral and immune system dynamics. *Nature Rev. Immunol.* 2(1): 28-36.
- Reece R, Michael A and Flanigan TP 2016 Immunity to Pathogens and Tumors *Encyclopedia of Immunology* 4: 355-362.
- Reluga T, Dahari H and Perelson A 2009 Analysis of hepatitis C virus infection models with hepatocytes homeostasis. *SIAM J. Appl. Math.* 69(4): 999-1023.
- Ribeiro RM, Lo A and Perelson AS 2002 Dynamics of hepatitis B virus infection. *Microbes Infect.* 4(8): 829-835.
- Smith AM and Perelson AS 2011 Influenza A virus infection kinetics: quantitative data and models. *Wiley Interdiscip. Rev.: Syst. Biol. Med.* 3(4): 429-445.
- Tseng CP and Chan YJ 2015 Overview of Ebola virus disease in 2014. *J. Chin. Med. Assoc.* 78(1): 51-55.
- Van den Driessche P and Watmough J 2002 Reproduction numbers and sub-threshold endemic equilibria for compartmental models of disease transmission. *Math. Biosci.* 180(1-2): 29-48.
- Wester T 2015 Analysis and simulation of a mathematical model of ebola virus dynamics. *Soc. Ind. Appl. Math.* 8: 236-256.
- WHO 1978 Ebola hemorrhagic fever in Sudan, 1976. *Bull. World Health Org.* 56(2): 247-270.
- WHO Ebola Response Team 2014 Ebola virus disease in West Africa—the first 9 months of the epidemic and forward projections. *New England J. Med.* 371(16): 1481-1495.
- Wong KK and Uyeki TM 2015 Clinical management of Ebola virus disease patients. *Curr. Treat. Opt. Infect. Dis.* 7(3): 248-260.